Conformational Analysis and CD Calculations of Methyl-Substituted 13-Tridecano-13-lactones

by **Elena Voloshina**[a])[1]), **Jörg Fleischhauer***[a]), and **Philip Kraft***[b])

[a]) RWTH Aachen, Institute of Organic Chemistry, Professor-Pirlet-Straße 1, D-52074 Aachen
[b]) *Givaudan Schweiz AG*, Fragrance Research, Überlandstrasse 138, CH-8600 Dübendorf

Conformational models covering an energy range of 3 kcal/mol were calculated for (13*S*)-tetradecano-13-lactone (**3**), (12*S*)-12-methyltridecano-13-lactone (**4**), and (12*S*,13*R*)-12-methyltetradecano-13-lactone (**8**), starting from a semiempirical Monte-Carlo search with AM1 parametrization, and subsequent optimization of the 100 best conformers at the 6-31G*/B3LYP and then the TZVP/B3LYP level of density-functional theory. CD Spectra for these models were calculated by the time-dependent DFT method with the same functional and basis sets as for the ground-state calculations and *Boltzmann* weighting of the individual conformers. The good correlation of the calculated and experimental spectra substantiates the interpretation of these conformational models for the structure–odor correlation of musks. Furthermore, the application of the *quadrant rule* in the estimation of the *Cotton* effect for macrolide conformers is critically discussed.

Introduction and Background. – Of the four different classes of musk odorants [1][2], that of macrocycles is the only one occurring in nature, and the authentic warm, sensual, and animalic odor of these compounds is much appreciated in perfumery. Despite their comparatively high price, they gained vital interest in recent years because of their good biodegradability [3]. Research has been focused on the development of less expensive routes to macrocycles and on the discovery of new, more-powerful musks to improve the price/performance ratio [1]. To smell musky, the macrocyclic ring must contain 14–18 members and a carbonyl, lactone, carbonate, or imino function as the *osmophore* to allow orientation and binding of the molecule at the receptor site. While gem-dimethyl substituents, or Et and higher alkyl groups generally strongly diminish the odor of macrocyclic musks, Me and methylidene substituents can intensify the musk odor [3]. Further elements in the molecular '*Lego set*' of macrocyclic musks are double bonds, and ether and thio-ether as well as carbonyl groups (*Fig. 1*). Especially these latter polar moieties need to be in well-defined positions in relation to the *osmophore* to intensify the musk note. For thiamacrolides, for instance, the odor threshold was significantly lowered when the S-atom was separated from the C=O group by four atoms in odd-membered rings (1,6-relation), and by five atoms (1,7-relation) in even-membered rings [1]. The two best macrocyclic musk odorants known to date are *(*R,Z*)-Nirvanolide*® (**1**; 0.05 ng/l air [4]) and (*R*,*Z*)-muscenone (**2**; 0.027 ng/l air [5]; *Fig. 1*), both possessing an (*R*)-configured Me-group-bearing C-atom and a (*Z*)-configured C=C bond as polar moiety.

For the design of new, even better-performing musks, we need to understand the influence these structural elements have on the odor of macrocycles, *i.e.*, we have to understand how they influence the conformational preferences of these highly flexible

[1]) Present address: *Max-Planck*-Institut für Physik komplexer Systeme, Nöthnitzer Straße 38, D-01187 Dresden.

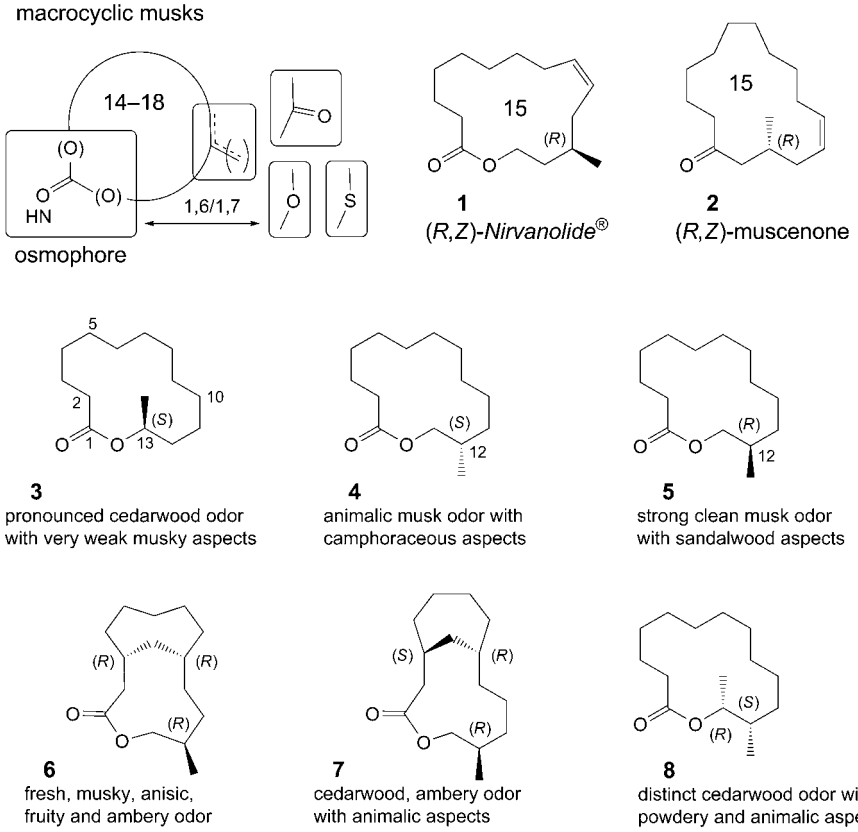

Fig. 1. *The structural parameters of musk odorants on the example of (*R,Z*)*-Nirvanolide® (**1**), *(*R,Z*)-muscenone* (**2**), *the Me-substituted tridecano-13-lactones* **3**, **4**, **5**, *and* **8**, *as well as the constrained macrobicycles* **6** *and* **7**

molecules. Most crucial in this respect are Me groups, which have a decisive influence on odor character and intensity, especially in the smaller rings. Prominent examples are the 14-membered methyl macrolides **3**, **4** and **5**, which occur in *Galbanum* [6] and *Angelica* root oil [7]. While (13*S*)-tetradecano-13-lactone (**3**) and its enantiomer *ent*-**3** possess a *pronounced cedarwood odor with only very slight musky character*, both enantiomers of 12-methyltridecano-13-lactone **4** and **5** smell musky, but differ significantly in their odor character [8]: The (*S*)-configured **4** has an *animalic musk odor with camphoraceous* aspects, the (*R*)-configured **5** a *strong clean musk odor with sandalwood aspects* (*Fig. 1*).

Constraining the conformational flexibility of **5** by introduction of a stereochemically-defined CH_2 bridge between C(3), and C(9) or C(8) led to the relatively rigid [7.5.1]- and [8.4.1]-bicycles **6** and **7** [9]. While the former one was *fresh musky in smell with anisic, fruity, and ambery side notes*, the latter bicycle **7** possessed again a *cedarwood, ambery odor with animalic aspects.* This was rationalized by a superposition analysis on the X-ray structure of *(4*S*,7*R*)-Galaxolide®* [10], in which **6** overlapped well, while the Me group of **7** protruded, so probably sterically hindered the interaction with

the musk receptor. Likewise, if the Me group in **3** and *ent*-**3** lies on the same *trans*-configured edge of the macrocycle as the C=O *osmophore*, it could hinder the interaction with the musk receptor and cause similar cedarwood odor profiles. In **4** and **5**, however, the Me substituent should rather be situated in a corner position or on a different side than the oxycarbonyl group, imitating rather a larger ring than hindering the interaction with the musk receptor. Introducing an ω-Me group in **4** indeed shifts the musk odor to a distinct cedarwood note [10]. But to substantiate these considerations, reliable conformational models for these highly flexible molecules are indispensable, *i.e.*, models that could be experimentally verified to some extent. The optical activity of the Me-substituted tridecano-13-lactones **3**, **4**, and **8** allows the comparison of experimental and calculated CD spectra, even when solvent effects are neglected. And since the *Cotton* effect depends critically on the molecular geometry, the accuracy of the calculated conformational space can be tested relatively precisely. In the following, we detail the conformational analysis and calculation of the CD spectra of the Me-substituted tridecano-13-lactones **3**, **4**, and **8**.

Results and Discussion. – *Conformational Analysis.* Starting from a local AM1 minimum, the conformational searches for **3**, **4**, and **8** was performed. This was carried out by the Monte-Carlo method[2]), employing the semiempirical AM1 parameterization [12] and the program Spartan [13]. The following eleven dihedral angles with increments of $\pm 120^\circ$ have been included in the search (see *Fig. 1* for numbering): $\theta_1 =$ C(3)–C(2)–C(1)–O(14); $\theta_2 =$ C(4)–C(3)–C(2)–C(1); $\theta_3 =$ C(5)–C(4)–C(3)–C(2); $\theta_4 =$ C(6)–C(5)–C(4)–C(3); $\theta_5 =$ C(7)–C(6)–C(5)–C(4); $\theta_6 =$ C(8)–C(7)–C(6)–C(5); $\theta_7 =$ C(9)–C(8)–C(7)–C(6); $\theta_8 =$ C(10)–C(9)–C(8)–C(7); $\theta_9 =$ C(11)–C(10)–C(9)–C(8); $\theta_{10} =$ C(12)–C(11)–C(10)–C(9); $\theta_{11} =$ C(13)–C(12)–C(11)–C(10).

Within an energy range of 10 kcal/mol, the 100 most-stable conformations were determined for each of the three molecules, and these were then optimized at the 6-31G*/ B3LYP level of density-functional theory[3]). Conformations within an energy range of 3 kcal/mol were further optimized [15] using a TZVP (Triple-ζ Valence plus Polarization) basis set [16] and the B3LYP exchange-correlation functional [17–19] (*Scheme*). Some selected dihedral angles of the resulting structures of **3a**–**3r**, **4a**–**4m**, and **8a**–**8m**, and their relative energies are given in *Tables 1–3*. The structures of the most stable conformers **3a**, **4a**, and **8a** are delineated in *Fig. 2*.

A recent conformational analysis of Me-substituted 14-membered macrocycles by DNMR spectroscopy and molecular-mechanics conformer search showed the prefer-

---

[2]) The Monte-Carlo method uses a standard simulated annealing algorithm (see http://pages.pomona.edu/~wsteinmetz/chem164/confsearch_spartan.doc; http://www.ugcs.caltech.edu/info/gsl/sian_1.html [11], with a temperature ramp of $T = T_f - \Delta T(1 - I/I_{max})^3$, where $\Delta T = T_f - T_i$, T_i and T_f are the initial and final temperatures, respectively, T is the current temperature; I and I_{max} are the current step number and the maximal number of steps, respectively, which depend on the number of the flexible centers of the studied molecule and the number of increments in the rotation. The new conformation is weighted *via* the *Boltzmann* criteria ($\exp(-\Delta E/(kT))$). In our calculations, we have used $T_i = 5000$ K, $T_f = 300$ K, and $I_{max} = 1089$.

[3]) The calculations have been carried out employing the GAUSSIAN 98 set of quantum-chemical routines [14].

Scheme. *Flow Chart of the Generation of the Conformational Models for (13*S*)-Tetradecano-13-lactone* (**3**), *(12*S*)-12-Methyltridecano-13-lactone* (***4***), *and (12*S*,13*R*)-12-Methyltetradecano-13-lactone* (**8**)

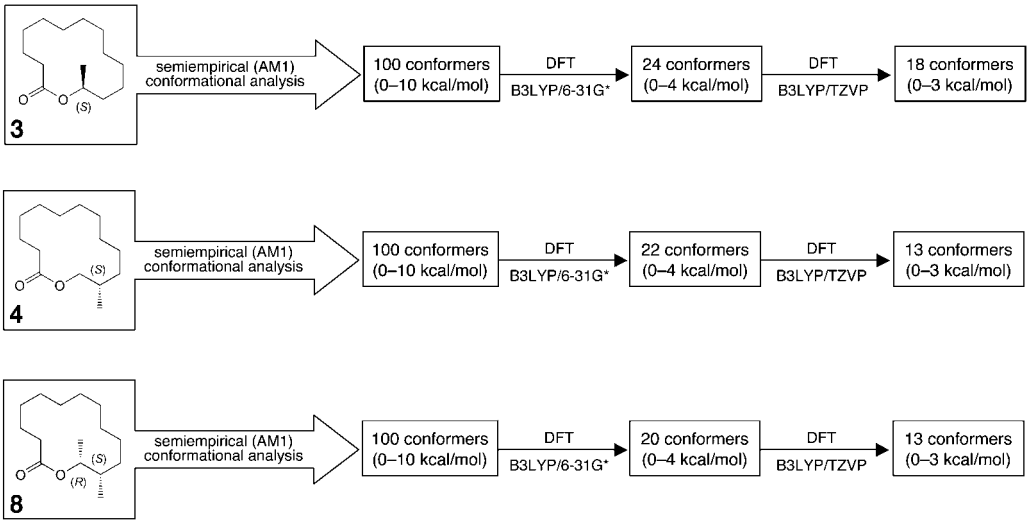

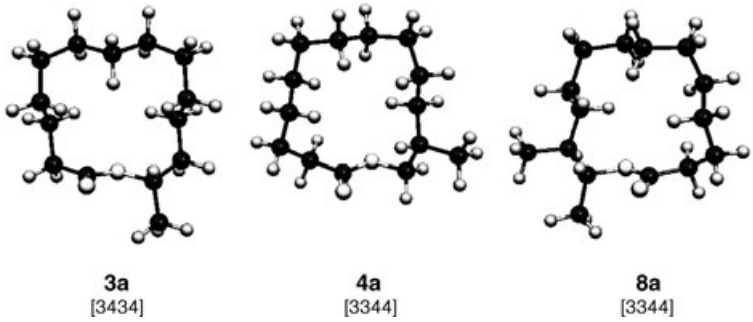

Fig. 2. *The structures of the lowest-energy conformers* **3a**, **4a**, *and* **8a** *of (13*S*)-tetradecano-13-lactone* (**3**), *(12*S*)-12-methyltridecano-13-lactone* (**4**), *and (12*S*,13*R*)-12-methyltetradecano-13-lactone* (**8**), *respectively*

ence for [3434] conformations as the lowest energy conformers, even in solution [20]. The conformations of macrocycles are designated according to the system of *Dale* [21], indicating, in square brackets, the number of bonds in the *trans*-configured edges of the macrocycles starting with the shortest *trans*-chain, and progressing in the direction of the next shortest – the sum of the numbers in the square brackets thus equals the ring size. Our calculations provided a [3434] conformation as the global energy minimum for **3** (**3a**; *Fig. 2*) as well as several other [3434] conformations among the 18 lowest-energy conformers (**3b**, **3c**, **3d**, **3e**, **3g**, **3j**, and **3r**). At the same time, the energy gap to the first [3344] conformer (**3f**) is just 0.64 kcal/mol. Surprisingly, in the case of the 12-

Table 1. *DFT-Optimized Geometric Parameters and Energies of the Conformers of* **3**

No.	Type	Geometry											*RE*[a])
		θ_1	θ_2	θ_3	θ_4	θ_5	θ_6	θ_7	θ_8	θ_9	θ_{10}	θ_{11}	
3a	[3434]	−77.094	−65.463	173.144	−57.557	−54.140	172.411	−171.253	55.618	55.538	178.446	66.291	0.00
3b	[3434]	−115.765	72.477	−163.976	178.985	−54.924	−59.446	175.175	−61.006	−57.229	176.881	−167.170	0.03
3c	[3434]	−58.207	−55.459	175.049	−168.166	61.081	63.977	−164.728	71.443	64.084	172.310	66.783	0.06
3d	[3434]	−48.073	−61.673	175.384	−174.212	59.836	63.661	−168.663	62.477	58.657	−173.229	167.658	0.25
3e	[3434]	−132.352	66.110	67.640	−177.881	64.198	60.713	179.736	59.210	48.631	62.068	−169.229	0.48
3f	[3344]	−143.128	64.904	67.114	176.929	69.911	74.525	−169.064	63.836	61.147	−168.227	166.471	0.64
3g	[3434]	−43.731	−61.733	174.205	−168.393	67.553	69.072	−167.175	96.612	−59.561	177.769	−177.372	0.76
3h	[3344]	−141.085	63.447	67.993	178.816	75.399	79.991	−170.545	100.853	−58.934	175.286	−169.451	1.07
3i	[3344]	−60.266	−60.932	173.505	−167.910	52.051	51.061	−168.333	164.653	−63.071	−65.503	172.138	1.51
3j	[3434]	−116.107	68.216	−175.669	−179.633	−58.985	99.308	−169.517	68.977	66.206	−168.250	166.689	1.56
3k	[3344]	−120.772	62.726	−177.988	178.601	−58.830	90.264	−161.472	168.057	−65.224	−65.214	174.780	1.81
3l	[3344]	−110.416	74.996	−162.310	179.241	−48.681	−53.742	167.484	−157.386	68.532	71.552	−170.393	2.11
3m	[3344]	−63.216	−64.948	174.567	−60.309	−52.145	−176.273	−170.395	97.108	−59.558	−66.852	−178.496	2.36
3n	[23333]	−70.570	−65.083	170.554	−73.983	−72.630	176.748	−72.630	−72.950	171.339	−72.394	−72.951	2.38
3o	[23333]	45.571	−152.112	71.507	70.918	−172.434	77.609	77.757	−171.131	75.971	75.520	−156.805	2.43
3p	[3335]	−102.721	64.205	178.153	172.718	−97.041	60.774	69.885	−179.705	77.207	82.351	−169.787	2.46
3q	[3335]	−148.837	95.996	−58.901	−66.255	−170.897	−59.008	−66.254	174.194	−73.190	−98.011	64.652	2.49
3r	[3434]	−113.023	68.590	72.719	−157.545	78.377	−160.777	172.256	−90.330	63.977	69.806	−170.923	2.94

[a]) Relative energy [kcal/mol]

Table 2. *DFT-Optimized Geometric Parameters and Energies of the Conformers of* **4**

No.	Type	Geometry											*RE*[a])
		θ_1	θ_2	θ_3	θ_4	θ_5	θ_6	θ_7	θ_8	θ_9	θ_{10}	θ_{11}	
4a	[3344]	−138.611	65.318	67.932	176.901	69.027	73.225	−170.939	64.434	62.057	−165.992	163.551	0.00
4b	[3344]	136.814	−65.667	−67.867	174.675	−64.266	−60.106	−176.983	−59.307	−50.669	−61.366	164.161	0.84
4c	[3434]	−112.632	68.076	−176.187	−178.605	−59.150	97.407	−169.828	69.689	67.251	−167.423	163.904	1.04
4d	[3344]	−118.008	62.726	−178.143	179.611	−58.983	89.792	−162.877	167.997	−66.787	−63.092	171.832	1.41
4e	[3344]	147.495	−65.966	−69.380	175.729	−74.618	−76.800	146.998	−75.821	172.999	173.186	58.435	1.66
4f	[3335]	−82.052	−59.785	−172.865	−66.150	−58.872	97.637	−171.685	−175.220	−54.047	−61.108	165.161	1.81
4g	[2444]	107.672	−64.219	174.904	−172.376	72.136	−138.656	69.102	69.344	−168.548	174.760	−58.177	1.82
4h	[3344]	46.140	68.594	−179.264	73.066	79.520	−167.599	101.064	−57.281	180.000	−174.850	67.949	2.16
4i	[3434]	−98.051	71.641	−167.201	−178.732	−51.057	−59.520	172.538	−92.036	75.213	−176.624	69.291	2.21
4j	[3335]	−63.630	−69.581	175.534	−77.433	−71.484	−175.843	−70.834	−60.224	106.765	−163.569	177.202	2.22
4k	[3434]	−147.149	67.175	72.270	−173.099	100.625	−61.418	177.769	−175.632	63.622	−111.640	161.499	2.30
4l	[3335]	133.109	−64.348	−72.748	151.269	−78.924	164.779	178.504	57.323	−96.583	171.000	−68.252	2.54
4m	[2345]	−121.857	57.694	65.441	−168.793	176.812	−65.214	−55.560	96.617	−173.665	−177.381	−66.005	2.98

[a]) Relative energy [kcal/mol]

Table 3. *DFT-Optimized Geometric Parameters and Energies of the Conformers of* **8**

No.	Type	Geometry											*RE*[a])
		θ_1	θ_2	θ_3	θ_4	θ_5	θ_6	θ_7	θ_8	θ_9	θ_{10}	θ_{11}	
8a	[3344]	149.006	−61.791	−65.639	171.939	−73.258	−74.981	171.263	−76.042	−71.995	−178.764	−64.139	0.00
8b	[3434]	95.137	−78.289	168.073	178.460	54.155	60.613	−174.264	62.785	59.355	−179.205	158.501	0.28
8c	[3344]	−135.728	−64.953	−68.744	179.201	−75.261	−77.352	173.365	−102.795	61.429	−173.388	161.927	0.98
8d	[3344]	130.849	−59.506	−60.006	177.020	−168.753	68.106	70.785	−143.606	76.068	−163.262	169.729	0.99
8e	[2444]	119.201	−64.161	171.332	−169.818	71.482	−136.184	69.113	70.734	−169.341	179.394	−61.102	1.66
8f	[3434]	119.516	−66.138	166.378	−175.932	56.523	−99.979	169.702	−79.844	−71.966	−173.835	−66.635	1.83
8g	[3434]	29.622	62.342	175.580	169.477	−66.955	98.750	−169.417	64.710	62.791	−172.429	160.587	1.96
8h	[3335]	72.548	65.323	−168.977	75.245	72.202	179.895	70.343	72.280	−166.071	73.285	74.428	2.20
8i	[3335]	153.451	−66.072	−71.360	169.185	−96.573	55.314	179.645	162.962	−78.935	157.794	−69.863	2.21
8j	[3434]	120.444	−66.202	178.909	179.114	59.283	−91.439	167.928	−141.902	73.169	−166.587	166.977	2.70
8k	[2435]	67.344	79.329	−67.627	−63.169	179.892	−178.382	59.060	63.703	−160.486	69.681	69.961	2.79
8l	[3335]	39.033	70.495	−177.834	75.152	80.078	−173.693	76.699	69.532	−104.508	−71.626	168.260	2.89
8m	[3344]	59.489	63.580	−176.759	86.379	−77.363	−178.231	−68.594	−64.837	93.323	−174.251	163.875	2.93

[a]) Relative energy [kcal/mol]

Me-substituted tridecano-13-lactones **4** and **8,** our calculations established [3344] conformers as being energetically most stable (**4a**, see *Fig. 2* and *Table 2*; **8a**, see *Fig. 2* and *Table 3*). The energy gap to the first [3434] conformer amounts to 1.04 kcal/mol (**4c**) and 0.28 kcal/mol (**8b**) in the case of **4** and **8**, respectively.

TDDFT Calculations. The CD spectra of the conformers **3a**–**3r**, **4a**–**4m**, and **8a**–**8m** have been calculated by the time-dependent DFT (TDDFT) method [15][22] using the same functional (B3LYP) and basis set (TZVP) as for the geometry optimization of the ground states. The rotational strengths have been calculated using the origin-independent dipole-velocity formulation [23]. The CD curves were obtained as a sum of Gaussians, each of which is centered at the calculated wavelength of the corresponding transition and multiplied with its rotational strength [24]. The Gaussians were generated with the empirical formula $\Gamma = k \cdot \lambda^{1.5}$ for the half bandwidth Γ at $\Delta\varepsilon_{max}/e$. The parameter k was set to 0.00375 [25], which yields a half bandwidth of *ca.* 10 nm at $\lambda \approx 215$ nm. The calculated CD spectra of the conformers were *Boltzmann*-weighted and added up to obtain the computed overall CD spectra for **3**, **4**, and **8**. The calculated and the measured CD spectra are shown in *Fig. 3*.

Our TDDFT calculations predicted the energetically lowest transition in the range between 210 and 220 nm in the CD spectrum for each conformer of **3**, **4**, and **8** (*Tables 4–6*). The transition occurs mainly from the n(HOMO) to the π^*(LUMO) of the carboxylic group. This transition results in positive *Cotton* effects ($\lambda_{calc.}(\mathbf{3}) =$ 217.2 nm, $\lambda_{calc.}(\mathbf{4}) = 215.8$ nm, $\lambda_{calc.}(\mathbf{8}) = 214.0$ nm) in the calculated CD spectra of **3**, **4**, and **8**, which correspond to the experimental ones [8][10] at 216, 216, and 214 nm, respectively[4]). The highest occupied and lowest unoccupied *Kohn–Sham* orbitals (KSOs) of the most stable conformers **3a**, **4a**, and **8a** are displayed in *Fig. 4*. The next calculated transition occurs at *ca.* 160 nm (not shown).

Application of the Quadrant Rule. Other than in the case of ketones, for which the *octant rule* has been widely accepted [27], several empirical sector rules were proposed for saturated lactones [28], taking more or less double-bond character of the O–CO single-bond into account [29][30]. However, judging from the *Kohn–Sham* orbitals in *Fig. 4*, this double-bond character is of very little importance, and lactones can be treated as C=O chromophores with *quasi*-C_{2v} symmetry. For these chromophores, a *quadrant rule* was proposed by *Schellman et al.* [31] to predict the sign of the $n \rightarrow \pi^*$ *Cotton* effect at *ca.* 220 nm. To test the practical usefulness of this rule, we predicted the *Cotton* effects of the different conformers also on the basis of the *quadrant rule.* In the quadrant diagram of the most-stable conformer **3a** (*Fig. 5*), the C-atoms C(1), C(2), C(13), and, in principle, also C(12) lie in the nodal plane defined by the lactone group, and, therefore, should not contribute to the overall *Cotton* effect of this conformer. Likewise, C(7) lies *quasi* on the perpendicular nodal plane, and should not contribute much either. C-Atoms C(3), C(4), C(5), and C(6) cancel with their positive contribution by and large the negative contribution of the atoms C(8), C(9), C(10),

---

[4]) We observed that TDDFT/B3LYP generally leads to a very good agreement with the experimental wavelengths, much better than for instance, the BP86-functional (see for example the calculations on calliactine [26]).

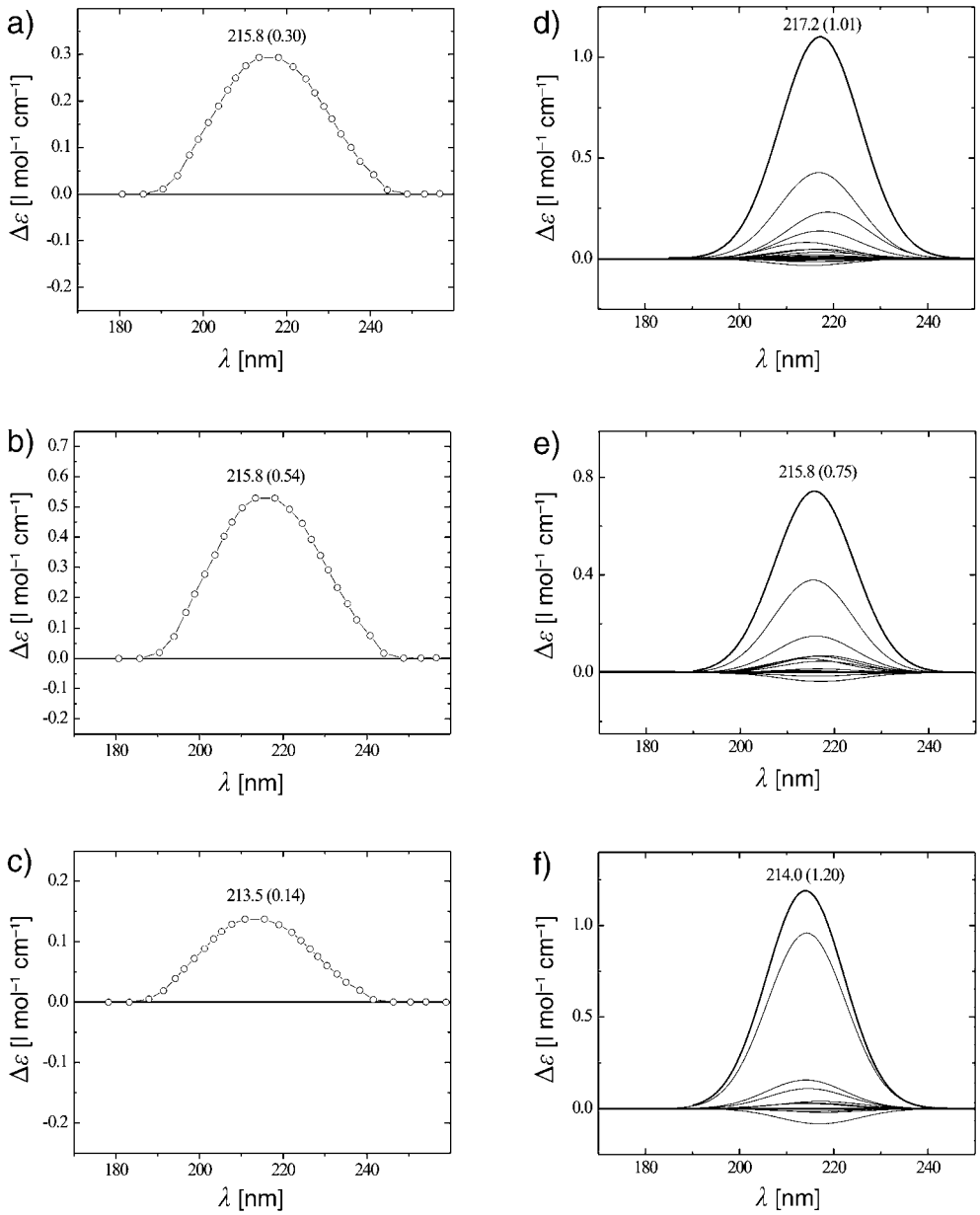

Fig. 3. *Comparison of the experimental CD spectra of* **3** (*a*), **4** (*b*), *and* **8** (*c*) *with the calculated ones at TZVP/B3LYP level of TDDFT for* **3** (*d*), **4** (*e*), *and* **8** (*f*). Thin lines in *d*, *e*, and *f* represent the individual spectra of the different conformers multiplied with the corresponding *Boltzmann* factor (*cf. Tables 4–6*).

Table 4. *The Electronic Configurations and Rotational Strengths for the Exited States of* **3** (transition 63 → 64, contribution typically > 95%). θ is the angle between the electric and the magnetic dipole moment[a]).

Conformer	Wavelength [nm]	θ [degree]	Rotational Strength [$\times 10^{-40}$ erg·cm^3]	$\Delta\varepsilon$ [l·mol^{-1}·cm^{-1}]	w_i[b]) [%]	$\Delta\varepsilon_w$[c]) [l·mol^{-1}·cm^{-1}]
3a	218.8	84.5	3.10	1.37	16.9	0.23
3b	214.3	86.3	1.13	0.50	16.1	0.08
3c	217.1	86.1	2.03	0.90	15.3	0.14
3d	216.9	71.8	8.66	3.85	11.4	0.44
3e	213.3	89.6	0.10	0.04	7.5	0.003
3f	215.2	84.0	1.82	0.81	5.7	0.05
3g	217.4	85.9	1.59	0.71	4.7	0.04
3h	214.9	104.4	− 4.35	− 1.94	1.7	− 0.03
3i	217.1	73.6	8.31	3.69	1.3	0.05
3j	216.2	78.2	3.83	1.71	1.2	0.02
3k	215.9	101.6	3.72	1.66	0.8	0.01
3l	215.2	77.9	3.42	1.53	0.5	0.008
3m	216.0	88.7	− 10.8	− 4.82	0.32	− 0.02
3n	216.2	89.2	− 9.66	− 4.30	0.31	− 0.01
3o	216.5	121.1	− 11.27	− 5.02	0.28	− 0.01
3p	215.2	74.8	4.95	2.21	0.27	0.006
3q	212.3	111.43	− 6.89	− 3.10	0.25	− 0.008
3r	215.0	105.1	− 2.74	− 1.22	0.10	− 0.001

[a]) In cases where this angle is close to 90° the sign of the corresponding *Cotton* effect is very sensitive even to small changes of the molecular structure. [b]) $w_i = \exp(-E_i/RT)/\sum_{i=1}^{N}\exp(-E_i/RT)$ is the *Boltzmann* factor of the i-th local minimum, where E_i is the energy of this local minimum, and N is the number of local stationary points. [c]) Influence of the individual conformers to the average spectrum: The $\Delta\varepsilon_{max}$ of the conformers multiplied with the corresponding *Boltzmann* factor.

Table 5. *The Electronic Configurations and Rotational Strengths for the Exited States of* **4** (transition 63 → 64, contribution typically > 95%)

Conformer	Wavelength [nm]	θ [degree]	Rotational strength [$\times 10^{-40}$ erg·cm^3]	$\Delta\varepsilon$ [l·mol^{-1}·cm^{-1}]	w_i [%]	$\Delta\varepsilon_w$ [l·mol^{-1}·cm^{-1}]
4a	215.53	83.2	1.51	0.67	56.3	0.38
4b	212.69	89.5	0.15	0.07	13.6	0.01
4c	216.01	80.3	3.49	1.49	9.7	0.14
4d	216.21	80.2	2.91	1.30	5.2	0.07
4e	214.15	79.4	3.78	1.72	3.4	0.06
4f	217.64	70.1	5.83	2.58	2.7	0.07
4g	215.95	92.6	− 1.20	− 0.54	2.6	− 0.01
4h	217.05	101.1	− 5.37	− 2.39	1.5	− 0.04
4i	216.47	84.9	2.55	1.13	1.4	0.02
4j	217.17	75.0	8.16	3.64	1.3	0.05
4k	213.39	88.3	0.58	0.26	1.1	0.003
4l	215.03	88.0	0.60	0.30	0.7	0.002
4m	215.95	89.1	0.33	0.14	0.4	0.0005

Table 6. *The Electronic Configurations and Rotational Strengths for the Exited States of* **8** (transition $67 \rightarrow 68$, contribution typically $> 95\%$)

Conformer	Wavelength [nm]	θ [degree]	Rotational strength [$\times 10^{-40}$ erg·cm^3]	$\Delta\varepsilon$ [l·mol^{-1}·cm^{-1}]	w_i [%]	$\Delta\varepsilon_w$ [l·mol^{-1}·cm^{-1}]
8a	214.24	74.91	4.77	2.13	44.9	0.96
8b	216.98	91.52	−0.67	−0.30	28.0	−0.08
8c	214.06	76.22	4.05	1.81	8.6	0.16
8d	214.58	80.09	2.91	1.30	8.4	0.11
8e	217.21	81.30	3.29	1.47	2.7	0.04
8f	215.25	79.83	3.45	1.54	2.0	0.03
8g	215.11	96.31	−2.04	−0.91	1.6	−0.01
8h	217.91	96.04	−3.78	−1.68	1.2	−0.02
8i	213.82	72.92	5.74	2.57	1.1	0.03
8j	214.05	85.69	1.21	0.54	0.5	0.003
8k	218.18	86.15	−4.75	−2.11	0.4	−0.008
8l	215.95	97.41	−2.91	−1.30	0.3	−0.004
8m	217.09	95.08	−2.58	−1.15	0.3	−0.003

and C(11) to the *Cotton* effect. The *pseudoequatorial* Me group, however, lies in a positive quadrant much closer to the C=O group than all other C-atoms do, and it, therefore, acts as a strong perturbator. Consequently, a positive *Cotton* effect is predicted in accordance with the calculated one ($\Delta\varepsilon = +1.37$ l/mol·cm). The situation is similar in the case of the conformers **3b**–**3g**, **3i**–**3l**, and **3p**. A negative *Cotton* effect was predicted for the energetically higher conformers **3m**–**3o**, and **3r** ($RE > 2$ kcal/mol; see *Table 2*), which is also in accordance with the calculations. However, for conformers **3h** and **3q** a positive *Cotton* effect was predicted, while calculated values of the rotational strengths have negative signs (**3h**: -4.35×10^{-40} erg·cm^3; **3q**: -6.89×10^{-40} erg·cm^3). On the whole, the *quadrant rule* predicts the calculated *Cotton* effects quite well in the case of (13*S*)-tetradecano-13-lactone (**3**), but, for the conformers of (12*S*)-12-methyltridecano-13-lactone (**4**; *Fig. 6*) and (12*S*,13*R*)-12-methyltetradecano-13-lactone (**8**; *Fig. 7*), the correspondence is less good. Discrepancies were observed for **4a, 4f**, **4j**, and **4k**, as well as for **8b**, **8g**, **8h**, **8i**, **8j**, and **8k**, respectively. These call the general applicability of the *quadrant rule* into question, though, for the majority of conformers, the *Cotton* effect was predicted correctly. In the application of the *quadrant rule*, attention has to be paid to *trans*-chains that are in immediate proximity oriented perpendicular to a nodal plane, such as in conformers **4c**, **4d**, and **4g**. There, they surpass the Me substituent in importance, and decisively influence the overall *Cotton* effect. Though, in general, the conformations of the macrocyclic ring of **8** resemble closer those of **4** than those of **3**, so are apparently more influenced by Me–C(12), the positions of Me–C(13) in the conformers of **8** are reminiscent to those of **3**, which could account for similar odor characteristics.

Interpretation and Conclusions. – Conformational models for the Me-substituted tridecano-13-lactones **3**, **4** and **8** were calculated and examined by calculation and correlation of the respective CD spectra with experimental data. In all conformers

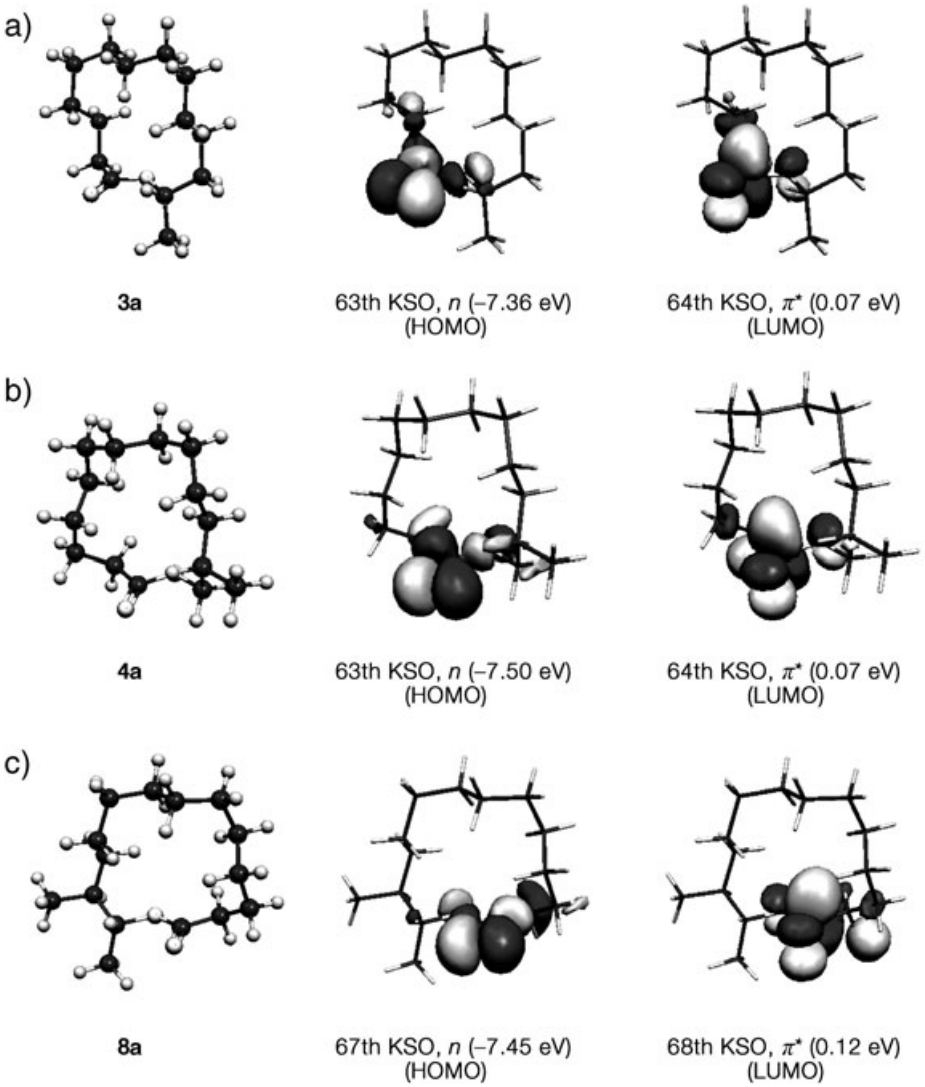

Fig. 4. Kohn–Sham *orbitals of the lowest-energy conformers* **3a** (*a*), **4a** (*b*), *and* **8a** (*c*)

considered, Me–C(13) of **3** and **8** is in *pseudoequatorial* conformation situated on the *trans*-edge that bears the C=O *osmophore*. This very well could hinder the interaction with the musk receptor, and would explain the *cedarwood* odor profiles of **3** and **8**. With the exception of conformers **4i** and **4m**, the Me substituent of **4** is, however, situated on a different side than the O–CO group. This should imitate a larger ring rather than hinder the interaction with the musk receptor. The good agreement of experimental and calculated spectra substantiates the validity of these models for the

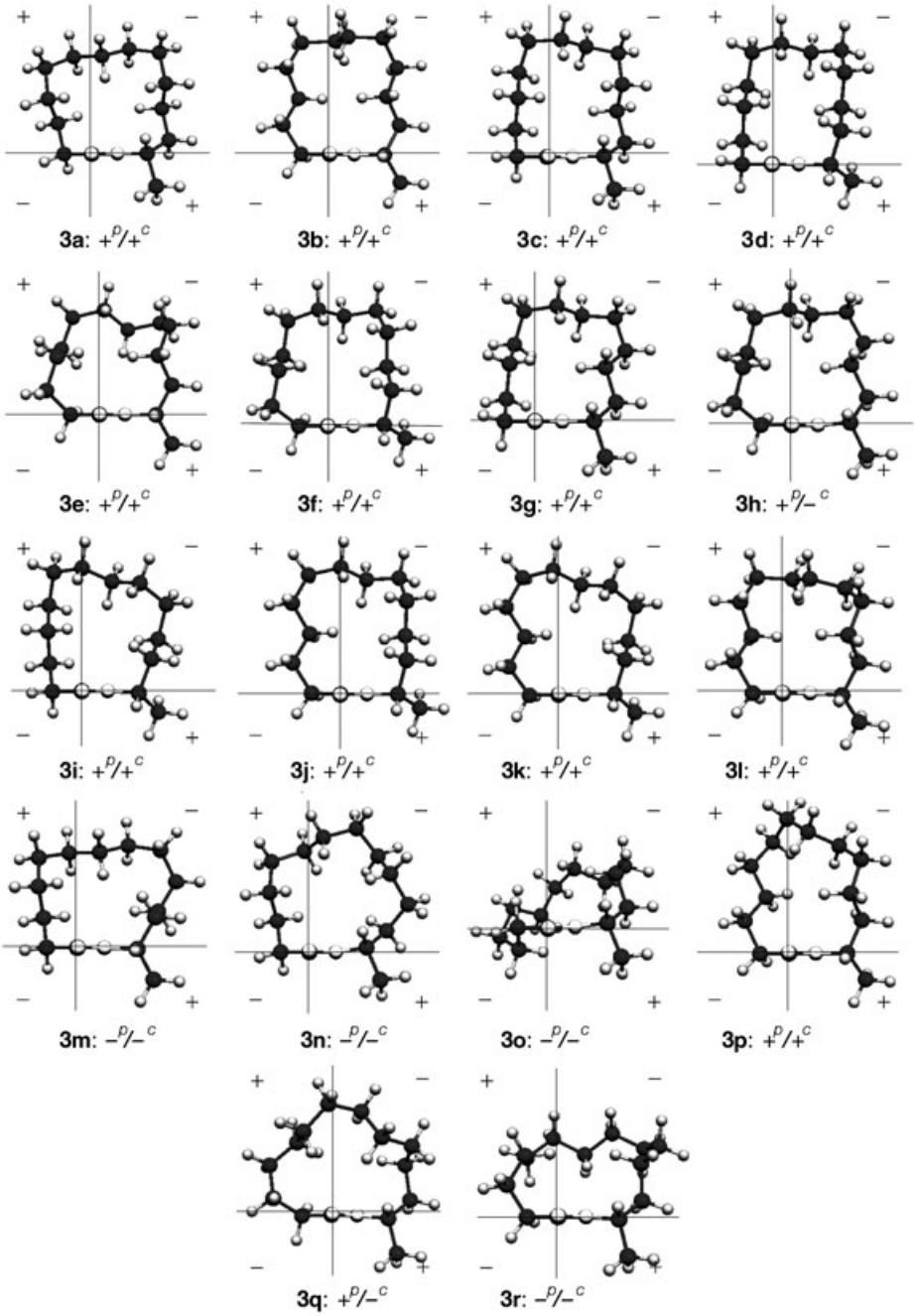

Fig. 5. *Quadrant diagrams of the conformers of (13*S*)-tetradecano-13-lactone* (**3**). The indices *p* and *c* indicate the predicted and calculated signs of the *Cotton* effect, respectively.

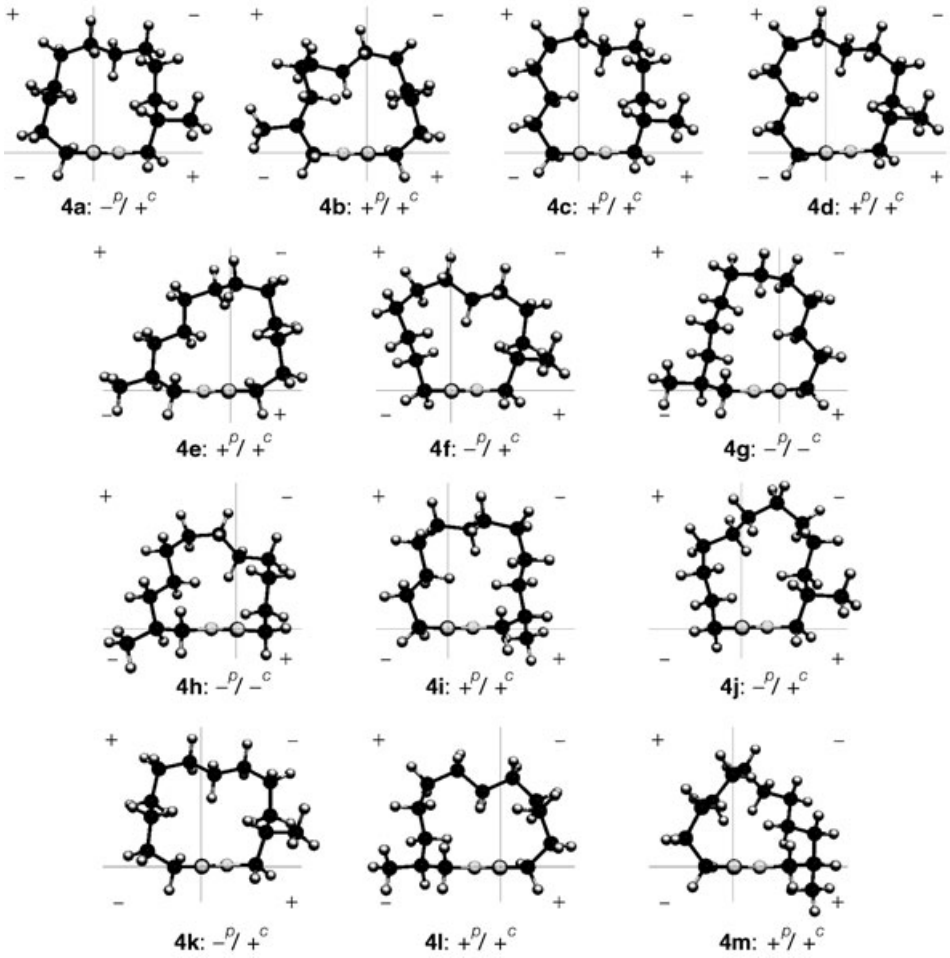

Fig. 6. *Quadrant diagrams of the conformers of (12*S*)-12-methyltridecano-13-lactone* (**4**). The indices *p* and *c* indicate the predicted and calculated signs of the *Cotton* effect, respectively.

interpretation of structure – odor correlations of these highly flexible molecules – and reliable conformational models are essential for molecular modeling. Caution is advisable in the application of the *quadrant rule* for estimating the *Cotton* effect for macrolides, although, for the majority of conformers, it predicts the sign correctly.

Proofreading of the manuscript by Dr. *Markus Gautschi*, Mr. *John Anthony M*^{c}*Stea*, and Ms. *Fanny Grau* is acknowledged with gratitude.

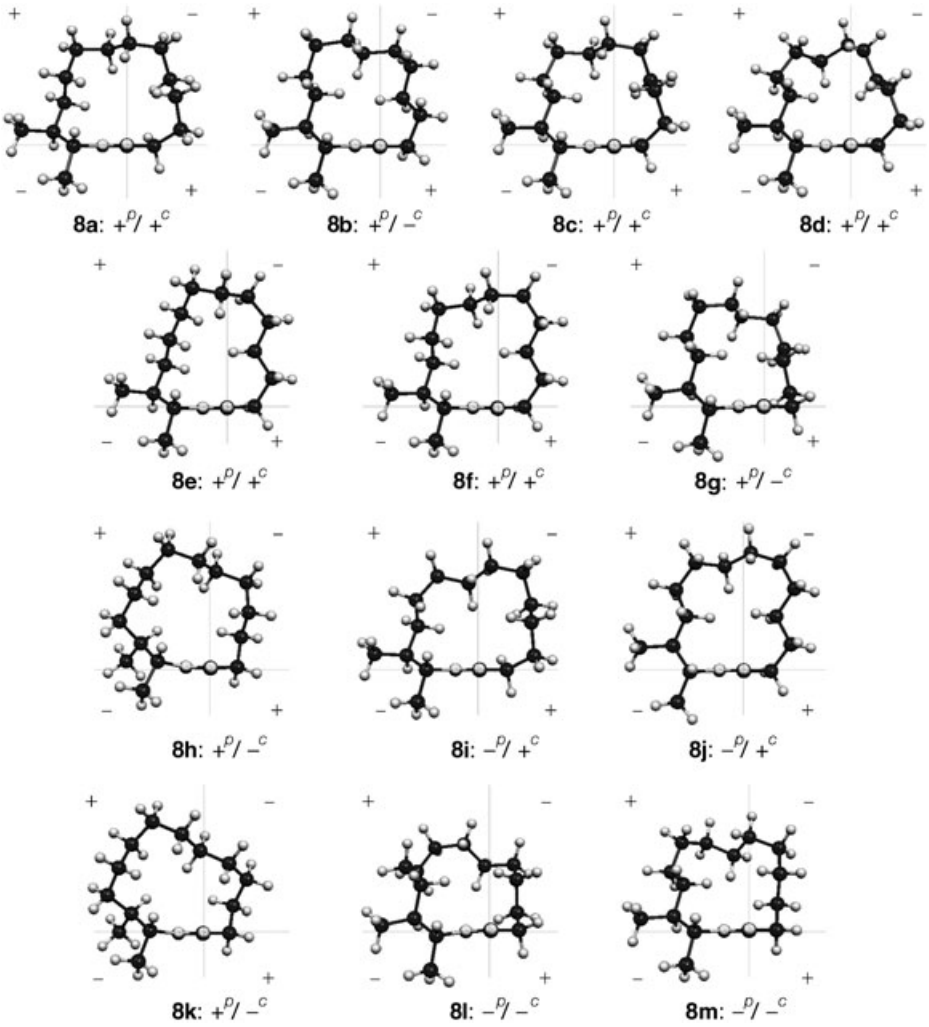

Fig. 7. *Quadrant diagrams of the conformers of (12*S*,13*R*)-12-methyltetradecano-13-lactone* (**8**). The indices *p* and *c* indicate the predicted and calculated signs of the *Cotton* effect, respectively.

REFERENCES

[1] P. Kraft, 'Aroma Chemicals IV: Musks', in 'Chemistry and Technology of Flavors and Fragrances', Ed. D. J. Rowe, Blackwell Publishing, Oxford, 2005, p. 143 – 168.
[2] P. Kraft, *Chem. Biodiv.* **2004**, *1*, 1957.
[3] P. Kraft, J. A. Bajgrowicz, C. Denis, G. Fráter, *Angew. Chem.* **2000**, *112*, 3106; *Angew. Chem., Int. Ed.* **2000**, *39*, 2980.
[4] P. Kraft, G. Fráter, *Chirality* **2001**, *13*, 388.
[5] C. Fehr, J. Galindo, O. Etter, *Eur. J. Org. Chem.* **2004**, 1953.
[6] R. Kaiser, D. Lamparsky, *Helv. Chim. Acta* **1978**, *61*, 2671.
[7] J. Taskinen, *Acta Chem. Scand., Ser. B* **1975**, *29*, 637; K. Schultz, P. Kraft, *J. Essent. Oil Res.* **1997**, *9*, 509.

[8] P. Kraft, W. Tochtermann, *Liebigs Ann. Chem.* **1994**, 1161; P. Kraft, W. Tochtermann, *Liebigs Ann.* **1995**, 1409.
[9] P. Kraft, R. Cadalbert, *Chem. – Eur. J.* **2001**, *7*, 3254.
[10] P. Kraft, W. Tochtermann, *Tetrahedron* **1995**, *51*, 10875.
[11] N. Metropolis, A. W. Rosenbluth, M. N. Rosenbluth, A. H. Teller, E. Teller, *J. Chem. Phys.* **1953**, *21*, 1087.
[12] M. J. S. Dewar, E. G. Zoebisch, E. F. Healy, J. J. P. Stewart, *J. Am. Chem. Soc.* **1985**, *107*, 3902.
[13] Spartan (Version 5.0), *Wavefunction, Inc.*, 18401 Von Karman Ave., Suite 370, Irvine, CA 92612, USA.
[14] Gaussian 98, Revision A.11, M. J. Frisch, G. W. Trucks, H. B. Schlegel, G. E. Scuseria, M. A. Robb, J. R. Cheeseman, V. G. Zakrzewski, J. A. Montgomery Jr., R. E. Stratmann, J. C. Burant, S. Dapprich, J. M. Millam, A. D. Daniels, K. N. Kudin, M. C. Strain, O. Farkas, J. Tomasi, V. Barone, M. Cossi, R. Cammi, B. Mennucci, C. Pomelli, C. Adamo, S. Clifford, J. Ochterski, G. A. Petersson, P. Y. Ayala, Q. Cui, K. Morokuma, P. Salvador, J. J. Dannenberg, D. K. Malick, A. D. Rabuck, K. Raghavachari, J. B. Foresman, J. Cioslowski, J. V. Ortiz, A. G. Baboul, B. B. Stefanov, G. Liu, A. Liashenko, P. Piskorz, I. Komaromi, R. Gomperts, R. L. Martin, D. J. Fox, T. Keith, M. A. Al-Laham, C. Y. Peng, A. Nanayakkara, M. Challacombe, P. M. W. Gill, B. Johnson, W. Chen, M. W. Wong, J. L. Andres, C. Gonzalez, M. Head-Gordon, E. S. Replogle, J. A. Pople, *Gaussian, Inc.,* Pittsburgh PA, 2001.
[15] TURBOMOLE (Version 5), R. Ahlrichs, M. Bär, H.-P. Baron, R. Bauernschmitt, S. Böcker, M. Ehrig, K. Eichkorn, S. Elliott, F. Furche, F. Haase, M. Häser, H. Horn, C. Huber, U. Huniar, M. Kattannek, C. Kölmel, M. Kollwitz, K. May, C. Ochsenfeld, H. Öhm, A. Schäfer, U. Schneider, O. Treutler, M. von Arnim, F. Weigend, P. Weis, H. Weis, Quantum Chemistry Group, University of Karlsruhe, Germany, 2004.
[16] A. Schäfer, C. Huber, R. Ahlrichs, *J. Chem. Phys.* **1994**, *100*, 5829.
[17] R. H. Hertwig, W. Koch, *Chem. Phys. Lett.* **1997**, *268*, 345.
[18] P. J. Stephens, F. J. Devlin, C. F. Chabalowski, M. J. Frisch, *J. Phys. Chem*. **1994**, *98*, 11623.
[19] http://www.cse.clrc.ac.uk/qcg/dft/def xc b3lyp.html.
[20] D. S. Clyne, L. Weiler, *Tetrahedron* **2000**, *56*, 1281.
[21] J. Dale, *Acta Chem. Scand.* **1973**, *27*, 1115.
[22] F. Furche, R. Ahlrichs, C. Wachsmann, E. Weber, A. Sobanski, F. Vögtle, S. Grimme, *J. Am. Chem. Soc*. **2000**, *122*, 1717.
[23] A. Moscowitz, in 'Modern Quantum Chemistry', Ed. O. Sinanoğlu, John Wiley & Sons, New York, 1965, Vol. 3, p. 21.
[24] J. A. Schellman, *Chem. Rev.* **1975**, *75*, 323.
[25] Y. Wang, G. Raabe, C. Repges, J. Fleischhauer, *Int. J. Quant. Chem.* **2003**, *93*, 265; G. Kurapkat, P. Krüger, A. Wollmer, J. Fleischhauer, B. Kramer, E. Zobel, A. Koslowski, R. W. Woody, *Biopolymers* **1997**, *41*, 267.
[26] E. N. Voloshina, G. Raabe, M. Estermeier, B. Steffan, J. Fleischhauer, *Int. J. Quant. Chem.* **2004**, *100*, 1104.
[27] D. A. Lightner, 'The Octant Rule', in 'Circular Dichroism', Eds. K. Nakanishi, N. Berova, R. W. Woody, 2nd edn., Wiley-VCH, Weinheim, 2000, p. 261 – 304.
[28] M. Legrand, M. J. Rougier, 'Application of the Optical Activity to Stereochemical Determinations', in 'Stereochemistry – Fundamentals and Methods', Ed. H. B. Kagan, Gerog Thieme Publishers, Stuttgart, 1977, p. 135 – 139.
[29] J. P. Jennings, W. Klyne, P. M. Scopes, *Proc. Chem. Soc. London* **1964**, 412.
[30] G. Snatzke, H. Ripperger, C. Horstman, K. Schreiber, *Tetrahedron* **1966**, *22*, 3103.
[31] J. A. Schellman, P. Oriel, *J. Chem. Phys.* **1962**, *37*, 2114; J. A. Schellman, *Acc. Chem. Res.* **1968**, *1*, 144; M. Keller, G. Snatzke, *Tetrahedron* **1973**, *29*, 4013.

Received September 28, 2004